ACS APPLIED MATERIALS & INTERFACES

Research Article

www.acsami.org

Ammonia-Sensitive Photonic Structures Fabricated in Nafion Membranes by Laser Ablation

J. L. Martinez Hurtado* and C. R. Lowe

Department of Chemical Engineering and Biotechnology, University of Cambridge, Cambridge CB2 1TN, U.K.

Supporting Information

ABSTRACT: Here we report the fabrication and characterization of photonic structures in Nafion membranes sensitive to ammonia in the 0.19%−12.5% concentration range. The photonic structures were recorded by laser ablation of silver nanoparticles synthesized in situ by diffusion. The particles showed an average diameter of 17 nm with a narrow size distribution. After ablation, the nanoparticles generated a diffracting structure giving colorful reflections at defined peak wavelengths. The reflectivity at these wavelengths was directly proportional to concentration after ammonia exposure. The concentration range that can be measured with these membranes encompasses the fatal limit of exposure and the lower flammable limit of gaseous ammonia. Interrogation by reflection spectroscopy makes them suitable for remote sensing and real-time monitoring of gases.

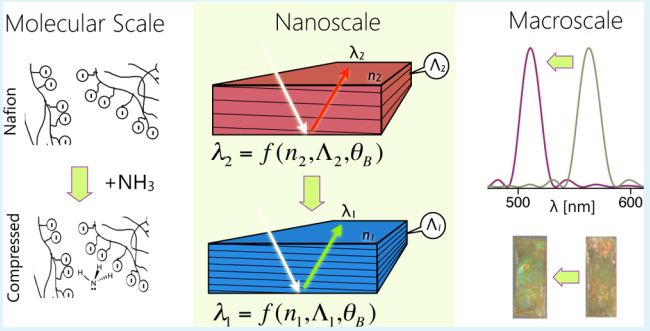

KEYWORDS: *ammonia, sensitive, photonic, laser, ablation*

1. INTRODUCTION

Gas sensors are widely used for monitoring environmental and industrial processes and have gained interest in biomedical applications and indoor environment control (e.g. automobiles, office spaces, laboratories). There is a plethora of commercially available sensors for diverse types of gases, which vary in concentration range and sensing mechanisms (e.g., semiconductors, infrared spectroscopy, combustion). Their main applications are fire control and indoor and industrial safety. Sensors for oxygen, hydrocarbons, H_2, H_2S, CO, and NH_3 are the most demanded types and account for 50% of the total market.[1] The most common gas sensing technologies utilize the reactivity of the analytes for sensing;[2] these sensors are nonreusable or have limited lifespans and have the disadvantage of analyte depletion or accumulation.[3] Recently, we have reported a holographic recording methodology for the fabrication of reversible hydrocarbon gas sensors without analyte depletion and without atmospheric gas interference.[4] The advantage of such sensors is that they can operate under adverse environmental conditions, such as high moisture. However, there is still a need for the reversible detection of reactive gases such as ammonia or oxygen. Here, we demonstrate the sensing of ammonia using a photonic structure embedded in a gas-sensitive material.

Ammonia sensors are essential for environmental monitoring, for the automotive and chemical industries, and more recently for biomedical diagnosis via breath analysis.[5,6] The presence of ammonia in breath can be indicative of renal failure, liver cirrhosis, and other medical conditions.[6−15] The ammonia concentrations in breath are in the parts per billion range, while for environmental or automotive applications concentrations lie in the parts per million range.[5] Ammonia detection for industrial safety requires, however, continuous monitoring of high concentrations in the percent range. Ammonia is explosive at concentrations higher than 15% (v/v) and fatal above 0.1% (v/v).[5] Electrochemical sensors cannot detect concentrations above the parts per million range without saturation; thus, there is a need for reversible ammonia sensors for these high concentrations. The ammonia sensor described in this work addresses concentrations within this range.

Photonic structures embedded in sensitive materials produce colorful reflections upon illumination with white light. The ordered diffraction of light is caused by the periodicity of the structure, and the wavelength and intensity depend solely on the geometry and optical properties of the materials. A layered structure with alternating refractive indices can be modeled by matrix methods using the periodic form of Maxwell's equations also known as the Block theorem.[16] The exact solutions can be calculated, and this method was used to analyze the data in this work (see Supporting Information for equations and model).

The reversible sensing of high concentrations of hydrocarbons using photonic structures has been recently reported.[4] Chemical-sensitive materials used in their fabrication report the presence of analytes due to interactions and perturbations in their molecular configuration. This results in bulk alterations of their geometry and optical properties, thus changing the

Received: March 19, 2014
Accepted: May 6, 2014
Published: May 6, 2014

   dx.doi.org/10.1021/am5016588 | ACS Appl. Mater. Interfaces 2014, 6, 8903−8908

reflected wavelength. These signals are read as changes in light intensity or wavelength shifts and are directly correlated with the concentration of the analyte causing the perturbations.[4]

Photonic structures are usually recorded in polymeric film materials by photo-induced reactions: metallic nanoparticles are formed in an ordered fashion by the energy differences in standing waves from laser light.[4] The inclusion of nanoparticles is achieved by diffusion of silver salts into the polymeric matrices, which are then transformed in situ into metallic nanoparticles. This well-known holographic recording technique requires translucent thin-film materials, and the resulting sensors are thus known as holographic sensors. Holographic sensors have been designed for a plethora of analytes in aqueous solutions,[17−27] gases, and volatile organic compounds.[4]

A great advantage of this type of sensor is their ability to measure gas concentrations reversibly in real-time.[1,4,28] A crucial step in the production of such sensors is finding compatible materials for both sensing and holographic recording. The materials should conform to the following criteria: form flat films, be translucent to laser light, allow for diffusion and formation of nanoparticles in their matrix, reversibly interact with the analytes, and change conformation or optical properties upon interaction. Here we report a methodology for the formation of photonic structures for the first time in a fluoropolymer material and its capabilities for sensing gaseous ammonia.

Ammonia is reactive due to its partial charges; materials that form reversible interactions with it are scarce. Proton exchange membranes are known to form reversible interactions with charged molecules in solutions, and thus we have exploited this property to form reversible interactions with gaseous ammonia. A readily available material that fulfills the requirements for the recording of a holographic sensor is the tetrafluoroethylene-perfluorosulfonic acid copolymer, Nafion. Nafion contains sulfonic acid groups inside its matrix that aggregate in continuous regions of ion clusters or cavities, allowing for gases and other molecules to permeate and form reversible interactions.[29−31] Mainly ionic interactions occur in these clusters and have been used for the loading of silver ions and in situ formation of nanoparticles.[32−34] The sulfonic charges of the cross-linked fluoropolymer provide the membrane not only with proton exchange capabilities but also with reversible interaction with positively charged molecules. Here we report the use of these properties for the detection of ammonia gas.

2. EXPERIMENTAL SECTION

Nafion N-117 membranes were purchased from AlfaAesar, U.K. The membranes were obtained in 15 cm × 15 cm thin films with 0.18 mm thickness. The membranes were sectioned in 8 mm × 22 mm strips and flattened down onto glass slides. The cation-selective transport only allowed cations to permeate, and thus the experimental process was adapted accordingly. After sectioning, the membranes were submerged into 50 mL of constantly stirred HNO_3 (68%) at 45 °C for 18 h to remove organic impurities from the manufacturing process.[35] Subsequently, the membranes were washed in constantly stirred deionized water at 50 °C for 25 min to remove excess acid and solubilized impurities. This step resulted in a change in coloration from a translucent yellowish to transparent colorless. The membranes were transformed into their ionic Na^+ form by soaking them in a 0.25 M NaOH solution for 24 h. After achieving equilibrium between sulfonic groups and sodium cations the membranes were washed in deionized water for 10 min, then transformed into the Ag^+ form by immersing them in 0.1 M $AgNO_3$ for 30 min to ensure 100% loading of Ag^+ ions.[33] The loading of the Ag^+ ions is limited by diffusion; thus, the ion concentration in the membrane can be controlled by loading

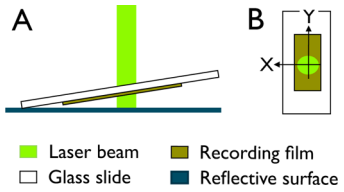

Figure 1. Schematic representation of the holographic recording of a photonic structure in a Nafion membrane. (A) The laser beam is directed through the flattened Nafion membrane, which acts as the recording film, then reflected back from a mirror surface facing the membrane. The standing waves ablate the embedded nanoparticles arranging them periodically. (B) The spot area was ellipsoidal with *X* and *Y* axes used to determine the optimal ablation area of 2.7 cm^2.

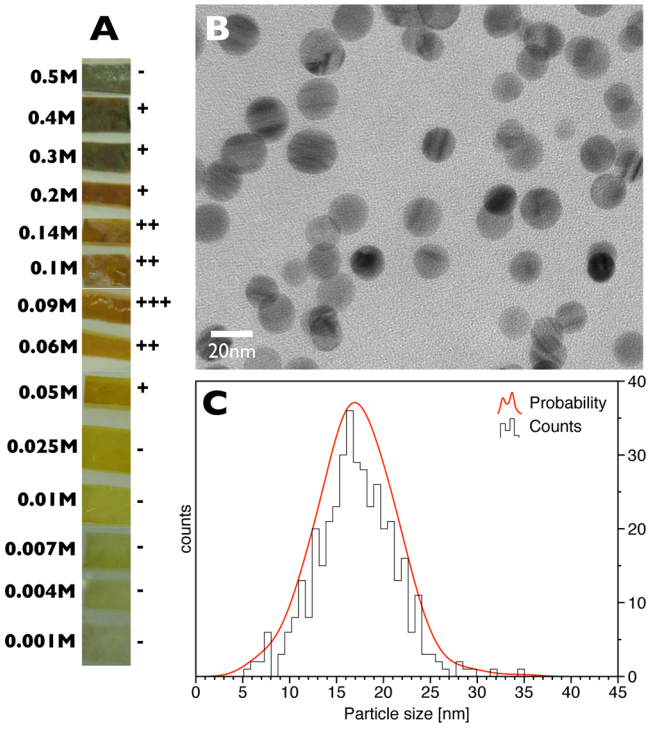

Figure 2. Size distribution and appearance of silver nanoparticles in Nafion membranes. (A) Nafion membranes containing different concentration nanoparticles corresponding to different $AgNO_3$ loading concentrations. The plus signs indicate those concentrations which produced monochromatic reflections after holographic recording by ablation. (B) TEM micrograph of a representative 0.09 M $AgNO_3$ loaded sample showing spherical silver nanoparticles. (C) Particle size distribution indicating an average particle size of 17 nm in diameter. No variation was observed with concentration, as the size is limited by the Nafion pore size.

time and concentration. The loading solutions were prepared keeping a 0.1 M $NaNO_3$ concentration constant and varying the amount of silver by changing the molarity of $AgNO_3$ between 0.001 and 0.5 M. Finally, the silver ions were transformed into metallic silver (Ag^0) by submerging them into a gently stirred 0.1 M $NaBH_4$ solution until the reduction process was completed (i.e., no further color change from transparent to yellow/amber). This step triggered the formation of nanoparticles up to 15 μm beneath the surface of the membranes.[34] This distance is necessary for the formation of the photonic structure layers.[1,28] Before holographic recording, the membranes were wiped with a wet tissue and kept hydrated in deionized water. To avoid nanoparticle formation on both sides of the membrane, one side was blocked with sticky adhesive putty (ethyl-cyanoacrylate resin) prior to the loading of silver. For faster fabrication and similar outcome, the

dx.doi.org/10.1021/am5016588 | ACS Appl. Mater. Interfaces 2014, 6, 8903−8908

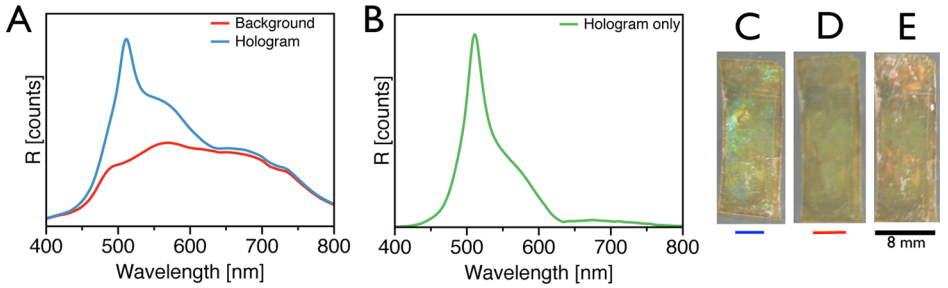

Figure 3. Monochromatic reflections from the photonic structures in Nafion membranes. (A) A typical reflection spectrum of a Nafion membrane containing a photonic structure, together with a background signal of the incident light. (B) Signal after subtracting the background. (C) Photograph of a Nafion membrane at the angle of incidence of the holographic reflections. (D) Membrane at an angle of no reflections similar to background in (A). (E) The membrane in (C) after exposure to water. The green reflections turn red upon exposure to water and the color variations are due to variations on the flatness during and after recording (see Supporting Information for time-resolved spectra).

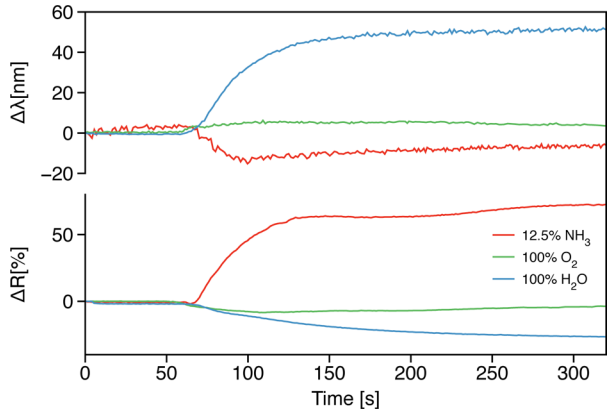

Figure 4. Exposure of the Nafion holograms to ammonia (12.5% v/v), oxygen, and water. The wavelength shift is plotted above, and the percentage change in reflectivity is plotted below. The water signal ($\Delta\lambda$ = 50 nm, ΔR = −25%) is greater than the oxygen signal ($\Delta\lambda$ = 6 nm, ΔR = −9%) which also decayed faster. Both signals incurred shifts in the same direction. Ammonia on the other hand showed a shift in the opposite direction ($\Delta\lambda$ = −14 nm, ΔR = 65%) with no interference from O_2 and H_2O.

membranes were exposed directly to 9:1 (v/v) ethanol−water solutions of $AgNO_3$ for 3 s, then washed with deionized water to stop the silver ion loading, and finally exposed to $NaBH_4$ solutions in 1:1 ethanol−water for 2 min. Using ethanol and methanol increases the swelling of the membranes and penetration of the solutions.[30] The nanoparticle formation and size distribution were corroborated by image analysis of micrographs (Fiji software) obtained with transmission electron microscopy. The Nafion membranes were embedded in epoxy resin and cut in 100 nm cross sections, mounted on Cu clip grids, and analyzed on a JEOL 200CX TEM.

A high-energy frequency-doubled Nd:YAG pulsed laser (Quantel, France) was used for the recording of photonic layers as previously reported elsewhere.[4] The methodology was adapted for Nafion membranes using an index matching liquid between a glass slide and the films for improved light transmission. The recording took place with the membranes facing the mirror opposite the direction of the laser beam as shown in Figure 1. The laser spot size was also varied to find the optimal ablation area with pairs X and Y dimensions of 1.2 and 1.4 cm, 1.7 and 1.9 cm, 1.8 and 1.9 cm, and 2.0 and 2.5 cm (see Figure 1B). An optimal ablation area is required to avoid surface effects caused by excess laser power. The inclination angle for the recording was kept fixed to 7°.

After recording, the membranes were placed in air-tight transparent flow-through cells designed for flattened samples and controlled gaseous environments. A flat-bed spectrophotometer (Avaspec-ULS2048-SLIT-25-VC, Avantes, U.K.) with a halogen white light source (Avalight-Hal-S, Avantes, U.K.) was used in reflection mode to detect the holographic reflections with a fixed angle of the light-guiding optical fibers at 25° (see Supporting Information). The resulting spectra were recorded and analyzed with the provided software (AvaSoft 7.2); peak wavelengths and peak light intensity were recorded over time. The exposure to gaseous ammonia was performed by injecting a 20 mL/min gas flow into the air-tight chamber for different concentrations of ammonia. The samples were exposed to concentrations ranging from 0.19% (v/v) up to 18% (v/v) of ammonia gas for 3 min. The logging of data was stopped after a maximum response was registered (i.e., equilibrium). After exposure, the samples were soaked in deionized water, blot-dried, and left to rest under room conditions for 18 h (23.5 °C, 40% RH) before reuse. The repeatability experiments consisted of 1 min recording of a baseline, 1 min exposure to a 1 mL/s gas flow of 0.19% (v/v) NH_3, and 20 min of exposure to air by opening the chamber to the atmosphere. The change in reflectivity ΔR was calculated as a percentile change of the peak reflectivity value for unexposed membranes compared to the peak reflectivity value after exposure (see Figure 3). $\Delta\lambda$ was calculated as the difference in peak wavelengths before and after exposure. For a given time after exposure there is a ΔR and $\Delta\lambda$ pair.

3. RESULTS AND DISCUSSION

The in situ formation of nanoparticles in Nafion membranes was successfully achieved by diffusion of $AgNO_3$ from solution. It was found that the content of silver particles in the membranes can be varied by changing the $AgNO_3$ concentration. The resulting membranes appeared semitranslucent with a yellowish to dark brown color indicative of nanoparticle formation (Figure A). Their presence and size were corroborated by TEM; they appeared spherical in shape with a narrow size distribution with ∼17 nm average diameter. Figure 2B shows a representative micrograph of the individual particles at high magnification; the size did not vary with concentration as it is limited by the Nafion porosity. Figure 2C shows the particle size distribution with minimum particle size of 5 nm and maximum of 35 nm.

The presence of nanoparticles beneath the surface is required for the absorption of laser radiation and formation of the photonic structure in Nafion. It was also required to form semitranslucent films for the laser light to be reflected through the membranes from the mirror surface. Not all concentrations tested yielded bright reflections; it was found that surface effects appear above 0.4 M $AgNO_3$, and no effect was observed below 0.05 M. Surface effects appear due to low light transmission through the film acting as a mirror with poor reflectivity; the result is poor transmission of nonmonochromatic multicolor reflections which are not useful for our study. Concentrations between 0.06 and 0.14 M, with optimal values around 0.09 M, produced bright monochromatic reflections

dx.doi.org/10.1021/am5016588 | ACS Appl. Mater. Interfaces 2014, 6, 8903−8908

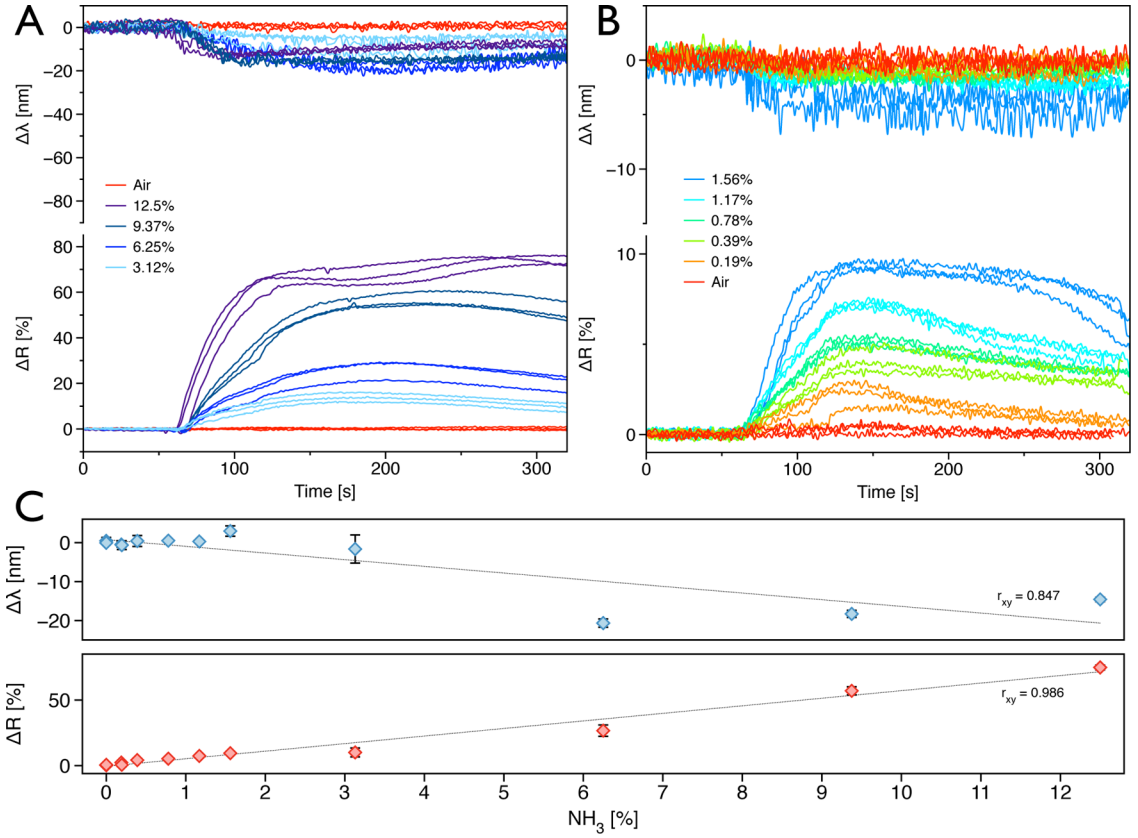

Figure 5. Response to high and low concentration of ammonia gas. (A) Peak wavelength and reflectivity signals recorded over time for high concentration of ammonia gas (3.12−12.5% v/v). (B) Peak wavelength and reflectivity for low concentration (0.19−1.56% v/v). The membranes were exposed continuously to the analytes after recording a 60 s baseline. The signal decayed after 120 s when the gas flow was stopped, and concentrations higher than 12.5% (v/v) resulted in deformation of the membranes. (C) Correlation curves for the maximum values of wavelength and reflectivity changes. Changes in reflectivity are in good agreement with changes in concentration (correlation coefficient for the linear fit r_{xy} = 0.986), whereas wavelength shift is not.

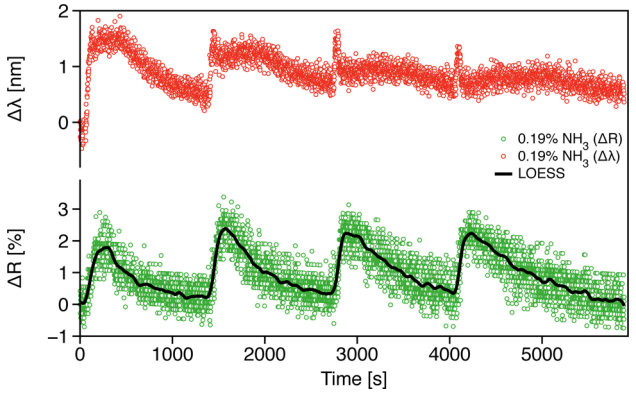

Figure 6. Repeating cycles of exposure to 0.19% (v/v) ammonia. The change in reflectivity showed repeatability with a recovery time of ∼1000 s. The change in wavelength was not repeatable. The black line corresponds to the local regression of the data points for Δ*R* over time.

suitable for sensing. Figure 2A shows images of the membranes fabricated with different amounts of silver, with the concentrations that generated monochromatic reflections indicated with a positive sign. Since 0.09 M loaded membranes produced the highest reflectivity, this concentration was chosen to construct samples for the rest of the characterization and gas exposure experiments. A laser spot area for ablation of 2.7 cm^2 with X = 1.8 cm and Y = 1.9 cm (see Figure 1) yielded the best results for the recording configuration and materials used.

The Nafion films containing photonic structures were flattened down onto glass slides and analyzed by reflection spectrophotometry. The samples showed a bright monochromatic reflection at around the wavelength of the recording laser (532 nm). Figure 3A shows the reflection signal together with the signal of the reference white light. By subtracting the background signal, it is possible to observe a relatively sharp peak from the monochromatic reflection of the photonic structure (Figure 3B). However, the signal is broad at the base due to the reflection of the normal coloration of the amber-colored membranes. Figure 3C shows photographs of a membrane and its characteristic green reflection at the satisfying angle of incidence.[4] Figure 3D shows the same membrane at a nonsatisfying angle where the reflections from the photonic structure cannot be observed due to their angular dependence (see ref 4).

To prove the sensing capability of the photonic structure, the membranes were exposed to water, oxygen, and ammonia. The peak position of the spectrum was monitored in intensity and wavelength, with the membranes being responsive to all three species as shown in Figure 4. The oxygen and water signal both resulted in a decrease in intensity and an increase of wavelength due to swelling.[4] Figure 3E shows a photograph of a membrane exposed to water proving a color shift to red (∼50 nm). Oxygen and water have the same effect on the membrane,

dx.doi.org/10.1021/am5016588 | ACS Appl. Mater. Interfaces 2014, 6, 8903−8908

although the oxygen signal is lower than the one for water (~5 nm) and thus oxygen concentrations could only be measured under controlled humidity conditions (see Supporting Information). Nevertheless, the response to ammonia could be clearly distinguished from oxygen and water and performed accurately under ambient humidity and oxygen concentrations; since all three components affect the response it is important to measure under constant environmental conditions. Figure 4 shows a large change in reflectivity and a small change in wavelength after exposure to ammonia. This was expected due to the contraction of the membranes by the interactions between ammonia and sulfonates inside the pores. The solubilized gas acts as a linkage, pulling the sulfonates together via electrostatic interactions; refractive index changes are also expected. The shrinking of the membrane causes the photonic structure to contract, thus decreasing the reflection wavelength and increasing the reflectivity.[4,36]

A systematic exposure to different gaseous ammonia concentrations was performed to test the sensitivity of the Nafion embedded photonic structures. A 60 s baseline was recorded followed by a 60s exposure to the different concentrations; Figure 5 shows the results. The maximum concentration detected was 12.5% (v/v), while above this concentration condensation of the gas caused the membranes to deform. The minimum concentration detected was 0.19% (v/v), limited by the sensitivity of the spectrophotometer. Changes in the reflectivity for a high concentration are plotted in Figure 5A and a low concentration in Figure 5B. The membranes were always kept at ambient conditions under atmospheric air with constant relative humidity; flushing with air did not have an effect on the signal.

A correlation exists between concentration and changes in reflectivity; wavelength shift also showed a correlation but not as satisfactory (Figure 5C). The sensitivity given by the error analysis of the data in Figure 5 corresponds to ~2% (v/v) for the high concentrations and ~2% (v/v) for the low concentrations. These values are large compared to other ammonia detectors; however, the sensor operates at very high concentrations usually not addressed by commercial detectors. To test the repeatability and reusability of the membranes, an experiment was conducted in which the membranes were left to equilibrate with the atmosphere after the ammonia exposure. The results for four cycles of the lowest detectable concentration are shown in Figure 6. The wavelength changes did not follow a repeatable trend, showing a permanent shift of 1 nm from the original value. Similar to the previous experiments, the membranes were exposed to the ammonia gas for 60 s after recording a 60 s baseline. The samples were left open to the atmosphere without airflow. It took over 20 min for the membranes to reach equilibrium again. Nevertheless, the reflectivity signal showed that these membranes can be used reversibly and repeatably for ammonia sensing. Ammonia sensors based on photonic structures have been reported elsewhere;[37,38] however, the detection mechanisms are either spectroscopic for gaseous samples[37,38] or based on chemical interactions for ions in solution.[39,40] The sensor configuration reported here directly addresses gaseous species via chemical interactions. Also, the concentration range detected by our sensor corresponds to levels at which ammonia is extremely dangerous and thus advantageous for safety monitoring. Furthermore, it offers the possibility of remote real-time analysis by measuring the colorful reflections, which in principle can be read by the eye, or a mobile phone, or any other photometric reader.[41]

4. CONCLUSIONS

For the first time, a methodology has been shown for recording photonic structures in Nafion, a gas-sensitive fluoropolymer. Silver nanoparticles with narrow size distribution and average diameter of 17 nm were produced in situ by diffusion of silver salts into the membranes. The recording of the photonic structure was achieved by ordered laser ablation of the embedded particles. The resulting photonic structure acts as a transducer for the gas−analyte molecular interactions and yields a signal which is monochromatic reflected light with varying wavelength and intensity. This ammonia sensor construct operates between 0.19% and 12.5% (v/v) ammonia, which are concentrations of great concern for human safety. The sensing properties of the membrane were characterized by reflection spectroscopy under ambient temperature and ambient humidity. The experimental results show that the sensor can be operated continuously and repeatably with notable accuracy.

■ ASSOCIATED CONTENT

Supporting Information

Photonic layer model and implementation in Mathematica, spectrophotometer setup details, time-resolved response to water, and sensitivity to oxygen gas. This material is available free of charge via the Internet at http://pubs.acs.org.

■ AUTHOR INFORMATION

Corresponding Author

*E-mail: jlm66@cantab.net.

Notes

The authors declare no competing financial interest.

■ REFERENCES

(1) Martinez-Hurtado, J. L.; Davidson, C. A. B.; Lowe, C. R. Monitoring Organic Volatiles and Flammable Gases with a Holographic Sensor. *Proc. SPIE* **2011**, *8024*, 80240Y−80240Y-7.

(2) Yamazoe, N.; Shimanoe, K. In *Science and Technology of Chemiresistor Gas Sensors*; Aswal, D., Gupta, S., Eds.; Nova Publishers: New York, 2007; pp 1−32.

(3) Comini, E.; Faglia, G.; Sberveglieri, G. *Solid State Gas Sensing*; Elsevier: New York, 2008.

(4) Martinez-Hurtado, J. L.; Davidson, C.; Blyth, J.; Lowe, C. Holographic Detection of Hydrocarbon Gases and Other Volatile Organic Compounds. *Langmuir* **2010**, *26*, 15694−15699.

(5) Timmer, B.; Olthuis, W.; van den Berg, A. Ammonia Sensors and Their Applications: A Review. *Sens. Actuators, B* **2005**, *107*, 666−677.

(6) Risby, T. H.; Solga, S. Current Status of Clinical Breath Analysis. *Appl. Phys. B* **2006**, *85*, 421−426.

(7) Marczin, N.; Yacoub, M. H. Disease Markers in Exhaled Breath: Basic Mechanisms and Clinical Applications. *Proc. NATO Adv. Study Inst.* **2002**, 346.

(8) Wells, K.; Vaughan, J.; Pajewski, T.; Hom, S.; Ngamtrakulpanit, L.; Smith, A.; Nguyen, A.; Turner, R.; Hunt, J. Exhaled Breath Condensate pH Assays Are Not Influenced by Oral Ammonia. *Thorax* **2005**, *60*, 27−31.

(9) Aguilar, A. D.; Forzani, E. S.; Nagahara, L. A.; Amlani, I.; Tsui, R.; Tao, N. A Breath Ammonia Sensor Based on Conducting Polymer Nanojunctions. *IEEE Sens. J.* **2008**, *8*, 269−273.

(10) Diskin, A. M.; Španěl, P.; Smith, D. Time Variation of Ammonia, Acetone, Isoprene and Ethanol in Breath: A Quantitative SIFT-MS Study Over 30 Days. *Physiol. Meas.* **2003**, *24*, 107.

(11) Smith, D.; Spanel, P.; Davies, S. Trace Gases in Breath of Healthy Volunteers when Fasting and After a Protein-Calorie Meal: a Preliminary Study. *J. Appl. Physiol.* **1999**, *87*, 1584−1588.

(12) Davies, S.; Spanel, P.; Smith, D. Quantitative Analysis of Ammonia on the Breath of Patients in End-Stage Renal Failure. *Kidney Int.* **1997**, *52*, 223−228.
(13) Narasimhan, L.; Goodman, W.; Patel, C. K. N. Correlation of Breath Ammonia with Blood Urea Nitrogen and Creatinine During Hemodialysis. *Proc. Natl. Acad. Sci.* **2001**, *98*, 4617−4621.
(14) DuBois, S.; Eng, S.; Bhattacharya, R.; Rulyak, S.; Hubbard, T.; Kearney, D. J. Breath Ammonia Testing for Diagnosis of Hepatic Encephalopathy. *Dig. Dis. Sci.* **2005**, *50*, 1780−1784.
(15) Shimamoto, C.; Hirata, I.; Katsu, K. Breath and Blood ammonia in Liver Cirrhosis. *Hepato-Gastroenterology* **2000**, *47*, 443.
(16) Pochi Yeh, A. Y. *Optical Waves in Crystals*; Wiley-Interscience: NY, USA, 1984; Chapter 6 Electromagnetic Propagation in Periodic Media, pp 155−219.
(17) Naydenova, I.; Raghavendra, J.; Martin, S.; Toal, V. *Humidity Sensors*; Nova Science Publishers, Inc.: Dublin, IE, 2011; Chapter 3. Holographic Humidity Sensors, pp 117−142.
(18) Sartain, F. K.; Yang, X.; Lowe, C. R. Holographic Lactate Sensor. *Anal. Chem.* **2006**, *78*, 5664−5670.
(19) Marshall, A. J.; Young, D. S.; Kabilan, S.; Hussain, A.; Blyth, J.; Lowe, C. R. Holographic Sensors for the Determination of Ionic Strength. *Anal. Chim. Acta* **2004**, *527*, 13−20.
(20) Kabilan, S.; Blyth, J.; Lee, M. C.; Marshall, A. J.; Hussain, A.; Yang, X.-P.; Lowe, C. R. Glucose-Sensitive Holographic Sensors. *J. Mol. Recognit.* **2004**, *17*, 162−166.
(21) Marshall, A. J.; Young, D. S.; Blyth, J.; Kabilan, S.; Lowe, C. R. Metabolite-Sensitive Holographic Biosensors. *Anal. Chem.* **2004**, *76*, 1518−1523.
(22) Marshall, A. J.; Blyth, J.; Davidson, C. A. B.; Lowe, C. R. pH-Sensitive Holographic Sensors. *Anal. Chem.* **2003**, *75*, 4423−4431.
(23) Mayes, A. G.; Blyth, J.; Millington, R. B.; Lowe, C. R. Metal Ion-Sensitive Holographic Sensors. *Anal. Chem.* **2002**, *74*, 3649−3657.
(24) Mayes, A. G.; Blyth, J.; Kyrlinen-Reay, M.; Millington, R. B.; Lowe, C. R. A Holographic Alcohol Sensor. *Anal. Chem.* **1999**, *71*, 3390−3396.
(25) Mayes, A. G.; Blyth, J.; Millington, R. B.; Lowe, C. R. A holographic sensor based on a rationally designed synthetic polymer. *J. Mol. Recognit.* **1998**, *11*, 168−174.
(26) Blyth, J.; Millington, R. B.; Mayes, A. G.; Frears, E. R.; Lowe, C. R. Holographic Sensor for Water in Solvents. *Anal. Chem.* **1996**, *68*, 1089−1094.
(27) Millington, R. B.; Mayes, A. G.; Blyth, J.; Lowe, C. R. A Holographic Sensor for Proteases. *Anal. Chem.* **1995**, *67*, 4229−4233.
(28) Martinez-Hurtado, J. L. Monitoring Volatiles and Flammable Gases without Electronics. *Nanotechnology* **2011**, *3*, 549−552.
(29) Huggings, R. A. *Advanced Batteries: Materials Science Aspects*; Springer: Standford, CA, USA, 2008; Chapter 14 Liquid Electrolytes, pp 325−328.
(30) Yeo, R. S. Dual Cohesive Energy Densities of Perfluorosulphonic Acid (Nafion) Membrane. *Polymer* **1980**, *21*, 432−435.
(31) Kreuer, K.-D.; Paddison, S. J.; Spohr, E.; Schuster, M. Transport in Proton Conductors for Fuel-Cell Applications: Simulations, Elementary Reactions, and Phenomenology. *Chem. Rev.* **2004**, *104*, 4637−4678.
(32) Rollins, H. W.; Lin, F.; Johnson, J.; Ma, J. J.; Liu, J. T.; Tu, M. H.; DesMarteau, D. D.; sun, Y. P. Nanoscale Cavities for Nanoparticles in Perfluorinated Ionomer Membranes. *Langmuir* **2000**, *16*, 8031.
(33) Sun, Y. P.; Atorngitjawat, P.; Lin, Y.; Liu, P.; Pathak, P.; Bandara, J.; Elgin, D.; Zhang, M. Nanoscale Cavities in Ionomer Membrane for the Formation of Nanoparticles. *J. Membr. Sci.* **2004**, *245*, 211−217.
(34) Sachdeva, A.; Sodaye, S.; Pandey, A. K.; Goswami, A. Formation of Silver Nanoparticles in Poly(perfluorosulfonic) Acid Membrane. *Anal. Chem.* **2006**, *78*, 7169−7174.
(35) Goswami, A.; Acharya, A.; Pandey, A. K. Study of Self-Diffusion of Monovalent and Divalent Cations in Nafion-117 Ion-Exchange Membrane. *J. Phys. Chem. B* **2001**, *105*, 9196−9201.
(36) Martinez-Hurtado, J. L. Elastic Holograms. *Proc. Interdiscip. Grad. Conf.* **2010**, *1*, 113−117.
(37) Ritari, T.; Tuominen, J.; Ludvigsen, H.; Petersen, J.; Sørensen, T.; Hansen, T.; Simonsen, H. Gas Sensing Using Air-Guiding Photonic Bandgap Fibers. *Opt. Express* **2004**, *12*, 4080−4087.
(38) Ozdemir, S.; Gole, J. L. The Potential of Porous Silicon Gas Sensors. *Curr. Opin. Solid State Mater. Sci.* **2007**, *11*, 92−100.
(39) King, B. H.; Gramada, A.; Link, J. R.; Sailor, M. J. Internally Referenced Ammonia Sensor Based on an Electrochemically Prepared Porous SiO2 Photonic Crystal. *Adv. Mater.* **2007**, *19*, 4044−4048.
(40) Kimble, K. W.; Walker, J. P.; Finegold, D. N.; Asher, S. A. Progress Toward the Development of a Point-of-Care Photonic Crystal Ammonia Sensor. *Anal. Bioanal. Chem.* **2006**, *385*, 678−685.
(41) Yetisen, A. K.; Martinez-Hurtado, J.; Garcia-Melendrez, A.; Vasconcellos, F. d. C.; Lowe, C. R. A Smartphone Algorithm with Inter-Phone Repeatability for the Analysis of Colorimetric Tests. *Sens. Actuators, B* **2014**, *196*, 156−160.